Short communication

Corrosion inhibition of Carbon Steel using a new morpholine-based ligand during acid pickling: Experimental and theoretical studies

Majid Rezaeivala [a,*], Mansoor Bozorg [b,*], Negar Rafiee [b], Koray Sayin [c], Burak Tuzun [c]

[a] Department of Chemical Engineering, Hamedan University of Technology, Hamedan 6516913733, Iran
[b] Faculty of Chemical and Materials Engineering, Shahrood University of Technology, Shahrood 3619995161, Iran
[c] Sivas Cumhuriyet University, Faculty of Science, Department of Chemistry, 58140 Sivas, Turkey

ARTICLE INFO

ABSTRACT

Here, a novel, relatively inexpensive Schiff base ligand (HL) has been studied as a corrosion inhibitor for the protection of steel in acidic solution. Different concentrations (0–25 ppm) of HL were added to the test solution and corrosion rate of steel and inhibition efficiency were determined. The obtained results indicated that HL is an efficient steel inhibitor in HCl solution and exhibits the maximum inhibition efficiency of 87.3 % at low concentration of 25 ppm. The EIS measurements revealed that polarization resistance increased from 319 Ωcm^2 to 2893 Ωcm^2, when the HL concentrations increased from 0 ppm to 25 ppm in HCl solution. Electrochemical experiments revealed that HL acted as a mixed type inhibitor, slowing both cathodic and anodic processes through adsorption which obeyed the Langmuir isotherm. The increase in inhibition efficiency up to 94.6 % with increase in immersion time up to 24 h was observed. Corrosion morphologies were observed by SEM to verify qualitatively the results obtained by electrochemical measurements. Quantum chemical calculations showed the preferred sites through which the molecules can interact with steel surface.

1. Introduction

Owing to its relatively high mechanical strength, low cost of production and abundance, mild steel has long been of interest in a wide range of industrial applications. However, this alloy suffers from corrosion in aggressive environments. Additionally, there are some unavoidable industrial processes, like industrial cleaning, acid scale removing and acid pickling in which HCl is used, which may also cause unwanted metal corrosion [1–5]. Corrosion has always been one of the main concerns of industrial users since it may result in huge economic loss and failure of components. Accordingly, great deals of effort have been made to overcome this phenomenon, including applying coatings and inhibitors onto the surface of the steel, and cathodic protection. The application of inhibitors is one of the simplest and most cost-efficient methods among the various methods used to control and minimize corrosion, [6–8]. Inhibitors are usually chemical compounds containing electron-rich atoms such as nitrogen, Sulfur, phosphorous and oxygen which contains conjugated π bonds and sometimes have aromatic rings. π bonds and electron-rich atoms provide the adsorption sites for these compounds to bind to the alloy surface [9–12]. Schiff base compounds containing the imine group (–C≡N-) have proven to act effectively as

corrosion inhibitors for metals in acidic media [13–16]. The key Schiff base condensation reaction, named after Hugo Schiff who first reported this type of reaction, simply involves the reaction of an amine with an aldehyde to eliminate water and give an imine [13]. Schiff bases, due to their high molecular mass, (C≡N) presence of groups with carbon and nitrogen double bonds and the pair of free electrons on the π atom, the existence of bonds. In addition, it has good inhibition efficiency in acidic environments [13]. Schiff base ligands and related complexes are used in a wide range of applications such as anti-corrosion [15], anti-cancerous [17], anti-bacterial and anti-fungal [18,19] applications, as well as being used as nanocatalysts [20,21] and chemosensors [22]. The present work aims to report the inhibitive effeciency of *2-((3-((2-morpholinoethyl)(pyridin-2-ylmethyl)amino)propylimino)methyl)naphthalen* assess the inhibitive potentiality of HL, a number of different experiments were performed. To evaluate the *−1-ol* (HL), a novel chemical compound as an inhibitor for mild steel corrosion in HCl solution. To corrosion inhibition effect, weight loss, polarization, and impedance tests were conducted while mild steel microstructures were recorded using SEM analysis. Theoretical calculations have also been carried out to provide additional detailed information of the activity of HL as an inhibitor molecule.

* Corresponding authors.

E-mail addresses: mrezaeivala@hut.ac.ir (M. Rezaeivala), M.bozorg@shahroodut.ac.ir (M. Bozorg).

2. Experimental

2.1. Materials

2.1.1. Specimen preparation

Mild steel specimens (composition (wt.%): 0.393C, 0.009 Al, 0.138 S, 0.024P, 0.009 Ti, 0.023 V, 0.012 Co, 0.079 Cr, 0.129 Ni, 0.561 Cu, 0.575 Mn, 0.032 Nb, 0.016 Mo, remainder Fe) were cut into desired dimensions for each test. To prepare a suitable surface, before each test, the exposed surface of the specimen was abraded and polished by SiC papers (100–1500).

2.1.2. Synthesis

N1-(2-morpholinoethyl)-N1-((pyridine-2-yl)methyl)propane-1,3-diamine was synthesized according to literature methods [17]. Formylpyridine, 2-hydroxy-1-naphthaldehyde, and 2-aminoethylmorpholine were purchased from Sigma Aldrich Company and used without further purification. IR spectra were recorded using the Alpha-BRUKER IR device. NMR spectra were recorded on a Varian Inova 500 MHz spectrometer operating at 500.06 MHz. Mass spectra were recorded on an Agilent Technologies (HP) 5973 mass spectrometer operating at an ionization potential of 70 eV. CHN analyses were carried out using a Perkin-Elmer, CHNS/O elemental analyzer model 2400 series 2.

2.1.3. Synthesis of 2-((3-((2-morpholinoethyl)(pyridin-ylmethyl)amino) propylimino)methyl)naphthalen-1-ol (HL)

N1-(2-morpholinoethyl)-N1-((pyridine-2-yl)methyl)propane-1,3-diamine (0.5 mmol, 0.139 g) in ethanol (20 mL) was added dropwise to stirring solution of *2-hydroxy-1-naphthaldehyde* (0.5 mmol, 0.086 g) in ethanol (50 mL). The mixture was stirred and refluxed for 12 h after which a brown oil was obtained which was collected, washed with cold ethanol and dried in vacuo.Yield: (88 %). Anal. Calc. for $C_{26}H_{32}N_4O_2$: C, 72.19; H, 7.46; N, 12.95. Found: C, 72.50; H, 7.33; N, 13.12 %. IR (ATR, cm^{-1}): 3424, 1633 υ(C=N), 1590, 1470 υ(C=C). EI-MS (*m/z*): 432.55, Found: 433.00 [L + 1]$^+$. ^{1}H NMR (CDCl$_3$, ppm) δ = 1.32 (s, 9H, H-r); 1.43 (s, 9H, H-w); 1.88 (p, 2H, H-f); 2.40 (t, 4H, H-b); 2.49 (t, 2H, H-e); 2.69 (t, 4H, H-c, H-d); 3.61 (t, 2H, H-g); 3.68 (t, 4H, H-a); 3.79 (s, 2H, H-i); 7.06 (d, 1H, H-k); 7.10 (t, 1H, H-m); 7.47 (t, 1H, H-s); 7.49 (s, 1H, H-p); 7.61 (t, 1H, H-l); 8.31(s, 1H, H-h); 8.51 (d, 1H, H-n); 13.81 (s, 1H, H-y). ^{13}C NMR (CDCl$_3$, ppm) δ = 29.28 (c-r); 29.43 (c-s); 31.32 (c-v); 31.52 (c-w); 28.46 (c-f); 51.47 (c-c); 52.08 (c-d); 54.08 (c-b); 56.99 (c-e); 57.16 (c-g); 60.94 (c-i); 66.91 (c-a); 117.80 (c-m); 121.85 (c-o); 122.83 (c-p); 125.67 (c-k); 126.68 (c-t); 127.84 (c-u); 131.85 (c-l); 136.33 (c-q); 148.91 (c-n); 157.80 (c-x); 160.14 (c-h); 165.96 (c-j) (Fig. 1).

2.1.4. Electrolyte

Using analytical reagent grade 37 % HCl, 1 M hydrochloric solution was made. The stock solutions were prepared in a 2:1 ethanol/HL
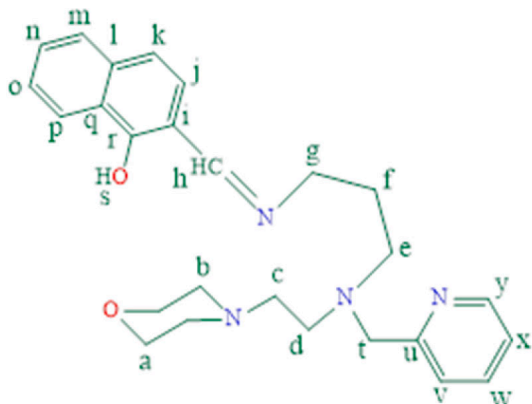

Fig. 1. Ligand HL.

mixture for complete solubilization with the following HL concentration: 0 (blank), 5 ppm (11.5 μM), 10 ppm (23.1 μM), 15 ppm (34.67 μM), 20 ppm (46.2 μM), 25 ppm (57.7 μM).

2.2. Methods

2.2.1 wt. loss method

The basis of other approaches is weight loss measurement, which is one of the most accurate ways for determining inhibitory efficiency. Three mild steel specimens were cut with dimensions of 5 cm × 2.5 cm × 0.2 cm. The cleaned and air-dried specimen were then accurately weighed and immersed in the test solution with different concentrations at a constant temperature of 25 °C, with and without HL, for 24 h. At the end of the immersion time the specimens were removed, their surfaces were carefully cleaned with ethanol according to ASTM G-31 [23] to remove the corrosion product, and then naturally dried. After that, the specimens were weighed to measure the weight loss, which was calculated by subtracting the weight of the specimens before and after immersion. The average weight of three specimens was used in the calculation in each case. The corrosion rates were determined before and after adding different concentration of HL. Using the following equations, the inhibition efficiency η_w(%) was calculated from the corrosion rate (CR) [24,25]:

$$CR = \frac{weight loss\,(mg)}{area\,(cm^2) time(h)} \tag{1}$$

$$\eta_w\% = \left(1 - \frac{CR}{CR^0}\right) \times 100 \tag{2}$$

Where CR^0 and CR are corrosion rates of mild steel (mg cm^{-2}h^{-1}) before and after adding the inhibitor in different concentrations, respectively. There is also a parameter as surface coverage (θ) defined to be:

$$\theta = \left(1 - \frac{CR}{CR^0}\right) \tag{3}$$

2.2.2. Electrochemical measurements

The inhibition impact of HL for mild steel corrosion was examined using electrochemical impedance spectroscopy (EIS) and the Polarization test approaches. To allow sufficient potential stability, the electrodes were immersed at an open circuit potential for 1 h before recording. The electrochemical cell involved a three- electrode set up in which working electrode (WE) was the mild steel specimen, auxiliary electrode (AE) was platinum electrode and reference electrode was saturated calomel electrode (SCE). All the EIS tests were conducted at OCP at frequency range of 100 KHz to 10 MHz with single amplitude perturbation of 5 mV. Potentiodynamic polarization (PDP) measurements were conducted by sweeping the potential in the range of −0.25 to + 0.25 V with 1 mVs^{-1} scan rate. Each of the tests was performed 3 times (Fig. 2).

2.2.3. Scanning electron microscopy

One molar HCl solution with and without HL in different concentrations was used to immerse the mild steel specimen for 24 h. Afterwards, the mild steel samples were carefully removed from the solution and cleaned using acetone. To investigate the morphology of specimen surface, SEM method was performed utilizing Zeiss Sigma 300-HV at 500 kV accelerating voltage and 2.5 Kx and 5 Kx magnifications.

2.2.4. Calculation method

The Gaussian software program was used to optimize the structure of the molecule HL [25] using the B3LYP and HF method 6–31++g(d, p) basis set. The quantum chemical parameters that were calculated included E_{HOMO}, E_{LUMO}, ΔE (HOMO-LUMO energy gap), electronegativity (χ), chemical potential (μ), chemical hardness (η), electrophilicity
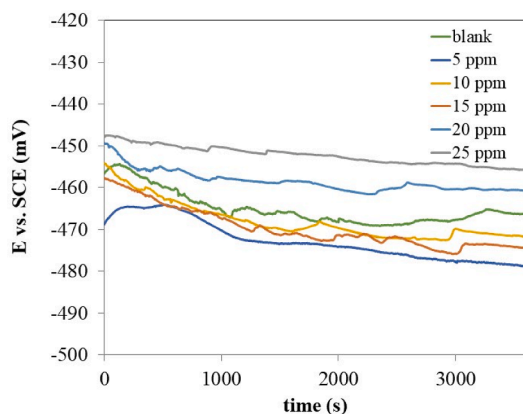
Fig. 2. Evolution of OCP for steel samples in 1MHCl solution containing different concentration of HL.

(ω), nucleophilicity (ε), global softness (σ) and proton affinity (PA) [24,26].

3. Result and discussion

3.1 Weight. loss test

The results of the mild steel weight loss experiment in 1 M HCl with and without HL are presented in Table 1. The experiment parameters of corrosion rate (CR) and surface coverage (θ) are calculated using equations (1) and (3), respectively. It is visible that when the inhibitor concentration increases, the corrosion rate decreases whereas the surface coverage increases, which shows that the increase of HL concentration results in an increase of adsorption. Table 1 also confirms the proportional relationship between inhibition efficiency (calculated according to Eq. (2)) and concentration of HL. When the concentration of HL reaches 25 ppm, the inhibition efficiency of HL was 87.3 % which indicates that HL is an effective corrosion inhibitor for mild steel corrosion in 1 M HCl solution.

3.2. Open circuit potential

The variation of open circuit potential (OCP) of mild steel versus SCE was investigated as a function of immersion time in acidic solution in the absence and presence of HL. Fig. 3 shows the obtained results. In blank solution, the OCP altered quickly towards more negative values, showing the initial dissolution process of the pre-immersion and the attack on the bare metal [27]. The displacement in OCP of the inhibited solutions are less than blank's solution. This results may be attributed to the delaying in dissolution action of mild steel by HL [28]. According to Riggs's theory and others [29–31], if the changes in OCP is more than ± 85 mV/SCE in relation to the corrosion potential of the blank, the inhibitor can be classified as a anodic or cathodic type, but the maximum shift in the presence of inhibitor is less than 25 mV/SCE, which shows that HL is a mixed-type inhibitor. Cao showed [32] if the shift in Ecorr is

Table 1
Results of weight loss measurement for mild steel in solution of 1 M HCl containing different concentrations of HL for 24 h at 25 °C.

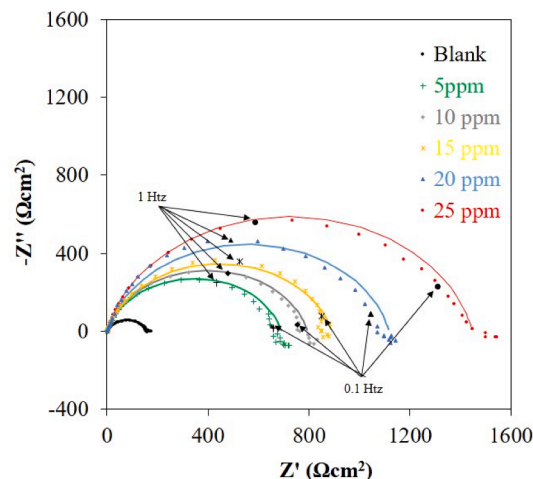| Concentration (ppm)	CR (mg/cm²h)	IE%	θ
0	0.10914	–	–
5	0.03182	70.81	0.708
10	0.02737	74.89	0.748
15	0.02199	79.83	0.798
20	0.01679	84.60	0.846
25	0.01382	87.32	0.873

Fig. 3. Nyquist diagram for mild steel in 1 M HCl solution in presence of different concentrations of HL.

negligible, the inhibition is most probably caused by blocking of active sites with the adsorbed inhibitor on the electrode surface.

3.3. Impedance test method

The Nyquist plots of EIS before and after adding different concentrations of HL are presented in Fig. 3. The shape of the plot is a compressed semicircle for all concentrations of HL which can be a sign of charge transfer resistance controlling the corrosion process. There is a visible increment in the diameter of the semicircular part of the Nyquist plot with the increasing concentration of HL, which shows that HL is an effective corrosion inhibitor in this case. A one-time constant electrical equivalent circuit shown in Fig. 4 was used to model the impedance plots and extract the electrochemical parameters. In this modeling, electrical circuit R_s, R_p and CPE are the solution resistance, total resistance or polarization resistance (R_p) and constant phase element, respectively. As it can be seen, the charge transfer resistance and constant phase element are both parallel and series to solution resistance. Different electrochemical parameters derived from EIS tests are presented as in Table 2. In this table, the chi-squared (χ^2) shows the square of the standard deviation between the fitting and the real data.. In other words, the lower value of (χ^2) indicates that the data which was fitted and the experimental data are in good agreement [33]. The values of χ^2 are on the order of 10^{-3}, which suggests the accuracy of the proposed equivalent circuits [34,35]. The inhibitory efficiency may be determined using the equation below in EIS measurements [36]:

$$\eta(\%) = \left(\frac{R_P - R_P^0}{R_P} \right) \times 100 \tag{4}$$

Where, R_P^0 and R_p are resistance of charge transfer before and after addition of inhibitor, respectively. Q and n are called CPE constant and CPE exponent which determines the phase shift, respectively. Parameter n can be used as a criterion of mild steel surface heterogeneity or roughness (0 < n less than 1) [37]. If n = 0, CPE represents a resistance and if n = 1 it represents a perfect capacitance with magnitude of Y.
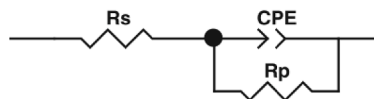

Fig. 4. One-time constant electrical equivalent circuit applied for the analysis of the impedance curves.

Table 2
Results of electrochemical impedance measurements for mild steel in 1 M HCl with different concentrations of HL.

C (ppm)	Q (μSs^{n}cm^{-2})	n	R$_p$ (Ωcm^2)	Chi-Square	C$_{dl}$ (μFcm^{-2})	τ (s)	η (%)
0	101.8	0.796	159.5	0.00797	1221.3	0.155	–
5	35.5	0.847	690	0.00811	220.7	0.152	76.88
10	32.3	0.848	793.5	0.00843	199.3	0.158	79.89
15	39.8	0.843	888.5	0.00387	279.9	0.249	82.04
20	27.2	0.851	1111.5	0.00957	166.0	0.184	85.65
25	35.0	0.876	1446.5	0.00388	162.4	0.255	88.97

However, a perfect capacitance behavior is unusual and CPE usually behaves as a combination of resistance and capacitance. The values of n seem to be related to a non-uniform current distribution because of roughness and surface defects. The double layer capacitance for a circuit comprising a CPE can be calculated using equation below [38]:

$$C_{dl} = Y^{\left(\frac{1}{n}\right)} R_P^{\left(\frac{1-n}{n}\right)} \tag{5}$$

Where Y is the magnitude of CPE. Capacitance is inversely proportional to the thickness of surface film according to the Helmholtz model for the surface absorbed film capacitance [39,40]:

$$C_{dl} = \frac{\varepsilon_0 \varepsilon}{d} S \tag{6}$$

where d is the thickness of film, S is the surface area of electrode, ε_0 is the air permittivity, and is the local dielectric constant. The data shown in Table 2 reveals a decrease in Cdl as the concentration of HL increases. This is most likely owing to a decreasing in the constant of local dielectric caused by the replacement of pre-adsorbed water molecules and/or a thickening of the protective layer created at the electrode surface. [41,42].

The relaxation time constant of a surface state is the time required for return of the charge distribution to equilibrium after an electrical disturbance, and in the case, when no distributed element is inserted to replace the double layer capacitance, it is calculated by using following equations [43,44]:

$$\tau = C_{dl} \times R_{ct}$$

In general, with increasing the inhibitor concentration, the time of the adsorption process becomes much higher, which attributed to a slow adsorption process [44,45]. According to Table 2, the addition of HL caused an increase in relaxation time constant values, therefore, the time of adsorption process becomes much higher which means a slow adsorption process.

According to Table 2, it can be clearly observed that as the concentration of HL increases, the value of R$_p$ increases as well. As it can be seen, the maximum value of R$_p$ (1446 Ωcm^2) is obtained when the concentration of HL reaches 25 ppm. This demonstrates that inhibitor molecules adsorbed on the mild steel surface have a larger surface coverage. The n values continue increasing as the concentration of HL reaches higher amounts contributed to the reduction of surface inhomogeneity and roughness as a result of the adsorption of inhibitor molecules.

3.4. Polarization test

The curves resulted from mild steel polarization tests are showed in Fig. 5, before and after the addition of 5–25 ppm of HL. As revealed by these plots, an increase in HL concentration has caused the curves to shift to the left. The study of these curves provides information about cathodic and anodic reactions. Recordings were conducted in Tafel mode and electrochemical parameters like corrosion potential (E$_{corr}$), corrosion density of current (i$_{corr}$), cathodic and anodic Tafel slope (βc and βα) and have been derived using extrapolation approach as shown in
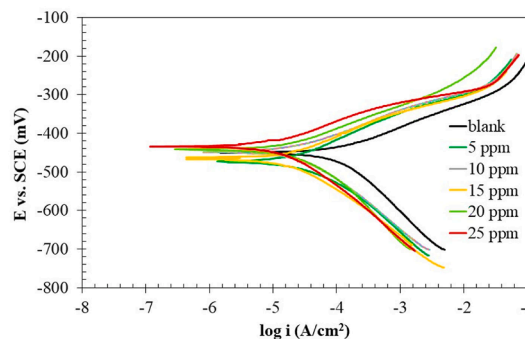
Fig. 5. Polarization curves for mild steel in 1 M HCl solution with different concentrations of HL.

Table 3
Polarization results of mild steel in 1 M HCl with different concentrations of HL.

Concentration of HL (ppm)	i$_{corr}$ (μA/cm^2)	E$_{corr}$ vs SCE (mV)	β$_\alpha$ (mV/dec)	β$_c$ (mV/dec)	η (%)
0	47.2	−450.7	32	68	–
5	13.0	−471.3	41	46	72.5
10	10.8	−447.3	30	51	77.1
15	8.16	−465.6	33	48	83.1
20	7.0	−455.4	34	53	85.2
25	5.8	−432.0	32	51	87.7

Table 3. By obtaining the values measured for i$_{corr}$ before and after addition of inhibitor, named i'$_{corr}$ and i$_{corr}$ respectively, the inhibition efficiency can be obtained using the equation below:

$$\eta(\%) = \left(1 - \frac{i_{corr}}{i'_{corr}}\right) \times 100 \tag{7}$$

The results demonstrate that the difference between the specimen's corrosion potential value in the presence and absence of inhibitor is less than 85 mV. Hence, the performance of HL as inhibitor has been a mix of anodic and cathodic. It is obviously observed that both anodic and cathodic curves shift to the lower current densities as the concentration of HL increases. It can also be seen that adding HL, up to the greatest value of 25 ppm, reduces corrosion current density, resulting in a rise in inhibition efficiency. This rise in efficiency is attributed to the anodic and cathodic inhibitory performance of HL adsorption on the mild steel surface, which blocks active sites on the mild steel surface. Both anodic and cathodic Tafel slopes change a little with augmented concentration of HL. It also indicates that HL could suppress both cathodic and anodic reactions, functioning as mixed-type inhibitors.

3.5. Adsorption isotherm

The surface coverage parameter (θ) must be collected to determine which adsorption isotherm best fits the behavior of HL on the mild steel surface. To describe the kind of interaction between mild steel surface and inhibitor molecules several models including Langmuir, Temkin,

Freundlich and Frumkin may be considered.

The equations related to these isotherms are as follows [46,47]:

$$\frac{C_{inh}}{\theta} = \frac{1}{K_{ads}} + C_{inh} \quad \text{Langmuir} \tag{8}$$

$$\frac{\theta}{1-\theta}\exp(-2\alpha\theta) = b \times C_{inh} Frumkin \tag{9}$$

$$\exp(-2\alpha a) = b \times C_{inh} Temkin \tag{10}$$

$$\log(\theta) = \log(K_{ads}) + n\log(C_{inh}) Freundlich \tag{11}$$

Where θ is the surface coverage, K_{ads} is the standard adsorption equilibrium constant and C_{inh} is the concentration of inhibitor. It was determined, from plots of C_{inh}/θ versus C_{inh}, that the best model for the interaction between HL and mild steel conforms to the Langmuir isotherm, giving a straight line with a slope of 1.0805 (Fig. 6). This shows that the adsorption of HL forms a secure monolayer on the mild steel surface resulting in an entirely smooth surface. For various metals, inhibitors, and acid solution systems, the Langmuir adsorption isotherm model has been widely employed in the previous study [31,48,49]. According to the Langmuir equation, it can be seen that the C intercept of diagram is equal to $1/K_{ads}$ and hence, the value of K_{ads} was calculated as follows:

$$\frac{1}{K_{ads}} = 0.0015 \rightarrow K_{ads} = 666 \tag{12}$$

Using the following equation, the standard Gibbs free energy of adsorption for HL was calculated [50]:

$$\Delta G_{ads}^{0} = -RTln\,(55.5\,K_{ads}) \tag{13}$$

where R is universal gas constant and the absolute temperature is represented by T. According to equation (13), the value of standard adsorption Gibbs free energy is −26.058 kJ/mol; therefore, it can be demonstrated that HL molecules have been adsorbed on the mild steel surface through a combination of chemical and physical adsorption process.

3.6. Effect of immersion time

The relation between both inhibition efficiency (η) and R_p with the immersion time for blank solution and 25 ppm of HL solution is presented in Fig. 7. It can be seen that when the immersion period is extended, the inhibition efficiency increases. For the blank solution, the values of R_p have decreased as the immersion time increases. However, for the 25 ppm of HL solution the values of R_p continues to increase with the increase of immersion time until 12 h, due to an increase in adsorption, but after 12 h it starts decreasing as a result of desorption. Still, as the amounts of R_p are also decreasing for the blank solution, it can be demonstrated that in presence of HL, the inhibition efficiency has increased.
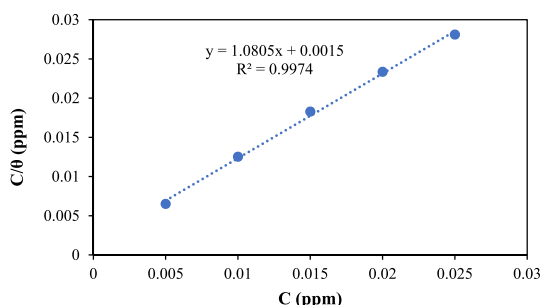

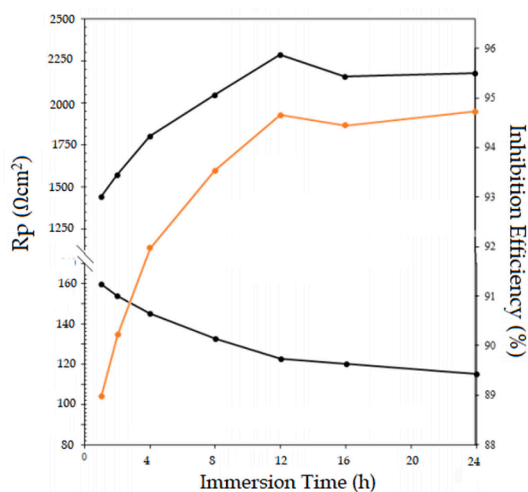**Fig. 6.** The plot of C/θ according to concentration in 25 °C.

Fig. 7. Rp against immersion time, as well as inhibition efficiency against immersion time plot for mild steel in 1 M HCl for a blank and 25 ppm of HL solution.

3.7. Scanning electron microscopy

Fig. 8 shows the specimen surfaces in solutions including different concentrations of HL. It is observed that surface of MS becomes clearer and cleaner with an increase in the concentration of HL. Pits are easily visible in blank specimens but there are only a few of them in the samples treated with 25 ppm of HL. Even the samples treated with 15 ppm of HL show less and a more uniform type of corrosion. It is clearly observed that the surface of samples is rough in the absence and smooth in the presence of HL. This indicates that HL performs well as a corrosion inhibitor for mild steel in HCl solution, notably in terms of minimizing pitting and cracking by adsorbing inhibitor molecules in the form of a layer on the mild steel surface.

3.8. Theoretical studies

Theoretical calculations were made to compare the inhibition activities of inhibitor molecules, generating a number of quantum chemical parameters about inhibitor molecules (Table 4 & 5). Among the quantum chemical parameters derived from theoretical calculations, the two most common parameters are HOMO and LUMO, which explain the inhibition by interacting chemically with an electron exchange.

The molecule with the highest HOMO energy numerical value of the inhibitor molecules has higher inhibitory activity. On the other hand, the molecule with the lowest LUMO energy numerical value of the inhibitor molecules has the highest inhibitory activity [39,51]. Given these two parameters, the inhibitory activity of the L molecule is higher. Apart from this, all parameters found as a result of the calculations are given in Table 4 and 5. The representations of the calculated parameters of the inhibitor molecules are shown in Fig. 9.

Apart from these parameters, another calculated parameter is the ΔE parameter, which is known to have high activity if the numerical value of this parameter is low [52]. The low value of this value facilitates electron transfer. Another parameter is electronegativity, which is the power of each of the atoms forming a bond to attract bond electrons, the numerical value of this parameter is known to have the highest activity of the smallest molecule [53].

Many properties of molecules are examined with the calculations made. Another calculated parameter is chemical hardness and softness, which are important parameters that express the measure of reactivity and stability [54]. Softness, which is the opposite of chemical hardness (1/η), expresses the polarization property of molecules. Soft molecules are more reactive than hard molecules as they readily offer electrons to

blank
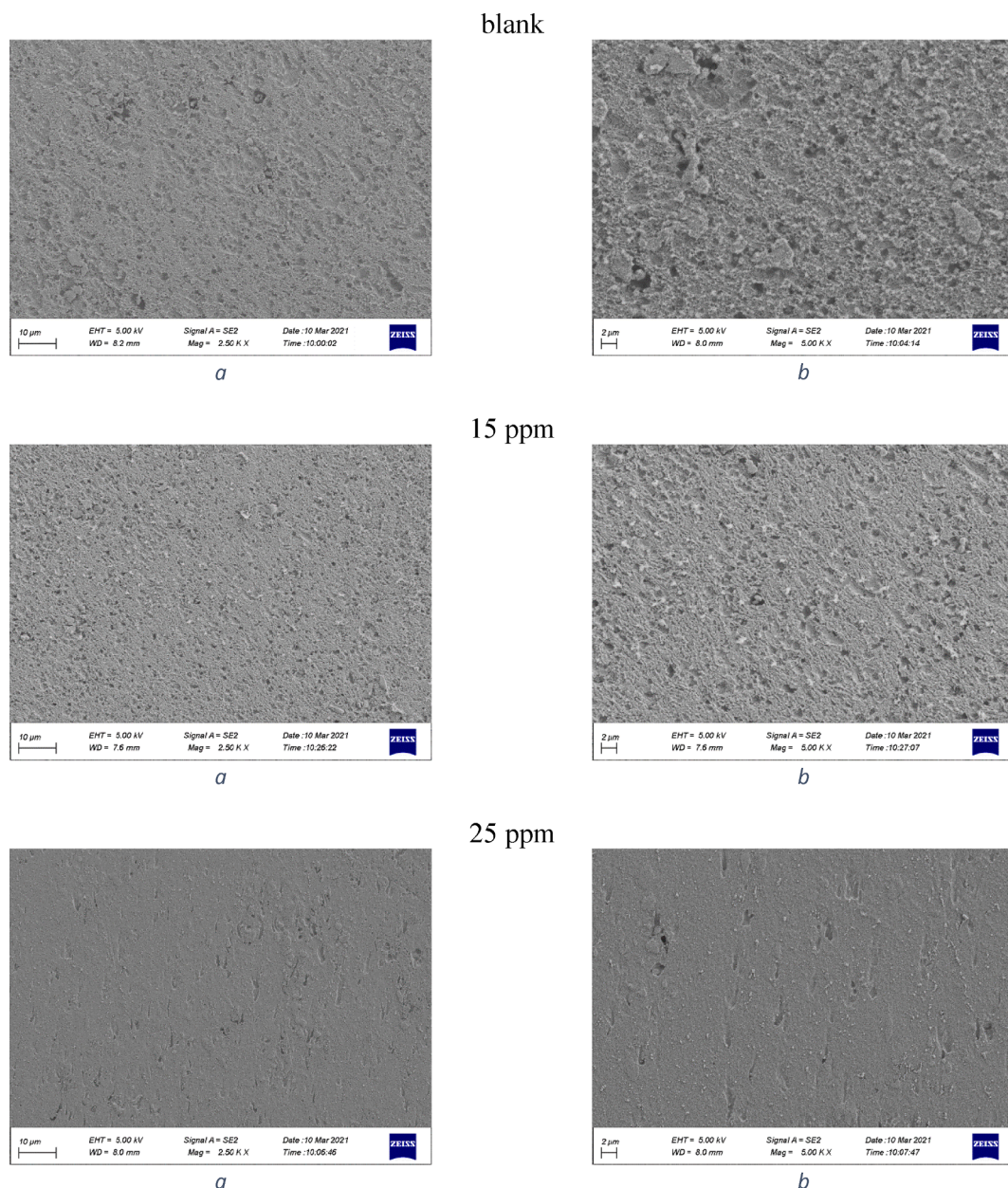
15 ppm

25 ppm

Fig. 8. SEM images recorded after immersion of mild steel samples in 1 M HCl before and after adding of 15 ppm and 25 ppm of HL in different magnification a) 2.5 Kx b) 5 Kx.

Table 4
The calculated quantum chemical parameters of molecules.

	E_{HOMO}	E_{LUMO}	I	A	ΔE	η	σ	χ	Pİ	ω	ε	dipol	Energy
B3LYP/6–31 g LEVEL													
L	−5.9210	−1.7505	5.9210	1.7505	4.1704	2.0852	0.4796	3.8357	−3.8357	3.5279	0.2835	3.7320	−37526.6582
HL'	−5.8440	−1.4471	5.8440	1.4471	4.3969	2.1984	0.4549	3.6455	−3.6455	3.0226	0.3308	2.3203	−37558.9455
HF/6–31 g LEVEL													
L	−7.9178	0.9598	7.9178	−0.9598	8.8775	4.4388	0.2253	3.4790	−3.4790	1.3634	0.7335	3.8903	−37286.8127
HL'	−7.9254	0.9399	7.9254	−0.9399	8.8653	4.4326	0.2256	3.4927	−3.4927	1.3761	0.7267	2.8953	−37317.9215

an acceptor molecule.

As a result of the theoretical calculations, many parameters were obtained. By using the numerical values of these parameters, inhibitory activity comparison can be made. In the calculations made, the numerical value of the HOMO parameter in the B3LYP method of the HL molecule is −5.8440, since this numerical value is higher than the other

molecule, its inhibitory activity is higher. On the other hand, the numerical value of the HOMO parameter in the B3LYP method of the HL molecule, from the protonated molecules obtained as a result of the protonation of the molecules, is −5.4040. Since this numerical value is higher than the other molecule, its inhibitory activity is higher. Likewise, the numerical value of the HOMO parameter in the HF method of

Table 5
The calculated quantum chemical parameters of protonated molecules.

|	E_{HOMO}	E_{LUMO}	I	A	ΔE	η	σ	χ	Pİ	ω	ε	dipol	Energy
B3LYP/6–31 g LEVEL													
L'	−5.5816	−1.3968	5.5816	1.3968	4.1849	2.0924	0.4779	3.4892	−3.4892	2.9092	0.3437	3.7167	−37090.9191
HL'	−5.4040	−0.9861	5.4040	0.9861	4.4178	2.2089	0.4527	3.1951	−3.1951	2.3107	0.4328	4.6502	−37123.1232
HF/6–31 g LEVEL													
L'	−10.180	−1.8417	10.180	1.8417	8.3385	4.1692	0.2399	6.0109	−6.0109	4.3331	0.2308	27.251	−36841.7485
HL'	−8.4889	3.3185	8.4889	−3.3185	11.807	5.9037	0.1694	2.5852	−2.5852	0.5660	1.7667	4.8841	−36878.9965
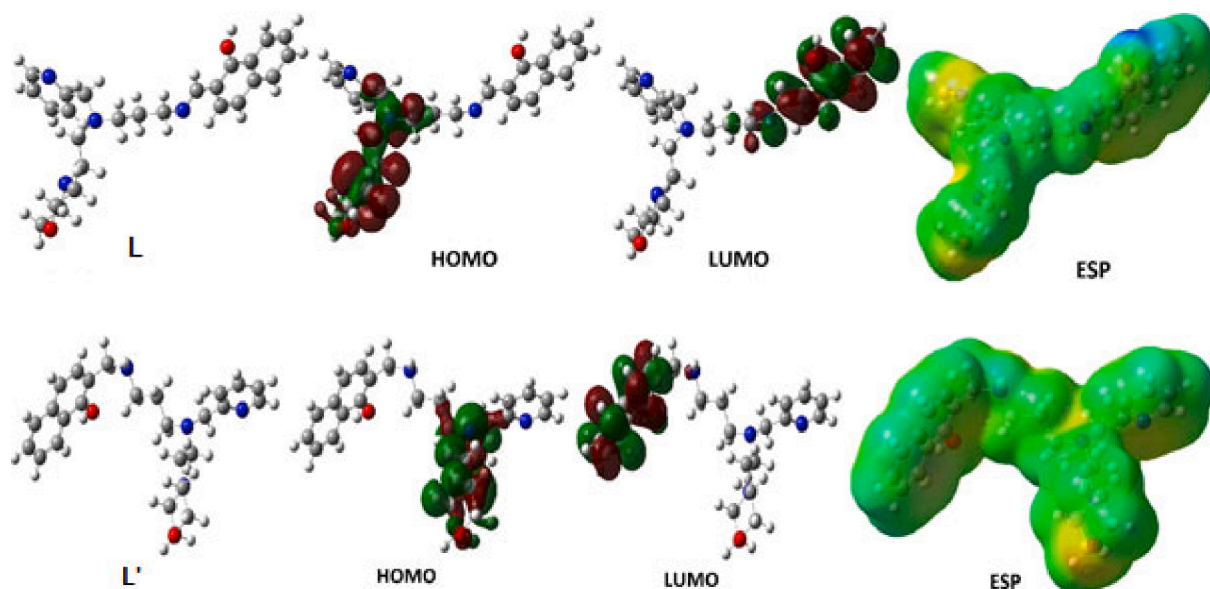
Fig. 9. Representations of optimized structures, HOMO, LUMO, and ESP shapes of inhibitor molecules.

the protonated HL molecule is −8.4889. The results of the numerical values of these parameters show that the experimental results have higher inhibitory activity of the HL molecule than the theoretical results for a great agreement.

4. Conclusions

1. In a 1 M HCl solution, HL acts as a great corrosion inhibitor against mild steel corrosion. Values of the inhibition efficiency were found to be proportional to the concentration of inhibitor.
2. The electrochemical tests show that HL molecules adsorb successfully at the metal-solution interface, with a mixed type of adsorption process.
3. According to EIS measurements, raising the concentration of HL increased the polarization resistance of the mild steel electrode (working electrode) while decreasing its capacitance.
4. The adsorption of HL on the mild steel surface obeyed the Langmuir adsorption isotherm and the value of ΔG^0_{ad} demonstrates that the adsorption was both physical and chemical.
5. SEM analysis justify that the presence of HL as an inhibitor reduces the corrosive effect and smoothened the surface of the mild steel specimen as compared to uninhibited medium.
6. Many quantum chemical parameters have been discovered as a result of theoretical calculations. Considering these parameters, it was seen that the inhibitory activity of the HL molecule was higher than the other molecule. Since the theoretical calculations are generally made in a pure and isolated environment, there is no solvent or experimental input. Therefore, there may be slight differences between the experimental results.

CRediT authorship contribution statement

Majid Rezaeivala: Conceptualization, Writing – review & editing. **Mansoor Bozorg:** Methodology, Writing – review & editing. **Negar Rafiee:** Data curation. **Koray Sayin:** Software, Investigation, Validation. **Burak Tuzun:** Software.

Declaration of Competing Interest

The authors declare that they have no known competing financial interests or personal relationships that could have appeared to influence the work reported in this paper.

Data availability

No data was used for the research described in the article.

References

[1] D. Guzmán-Lucero, O. Olivares-Xometl, R. Martínez-Palou, N.V. Likhanova, M. A. Domínguez-Aguilar, V. Garibay-Febles, Synthesis of selected vinylimidazolium ionic liquids and their effectiveness as corrosion inhibitors for carbon steel in

aqueous sulfuric acid, Ind. Eng. Chem. Res. 50 (2011) 7129–7140, https://doi.org/10.1021/ie1024744.

[2] S.D. Shetty, P. Shetty, H.V. Sudhaker Nayak, The inhibition action of N-(furfuryl)-N′-phenyl thiourea on the corrosion of mild steel in hydrochloric acid medium, Mater. Lett. 61 (2007) 2347–2349, https://doi.org/10.1016/j.matlet.2006.09.009.

[3] K. Kiruthikajothi, G. Chandramohan, Corrosion inhibition of mild steel in hydrochloric acid solution by amino acid complexes, Orient. J. Chem. 31 (2015) 1351–1354, https://doi.org/10.13005/ojc/310312.

[4] J. Hmimou, A. Rochdi, R. Touir, M. Ebn Touhami, E.H. Rifi, A. El Hallaoui, A. Anouar, D. Chebab, Study of corrosion inhibition of mild steel in acidic medium by 2-propargyl-5-p-chlorophenyltetrazole: Part I, J. Mater Environ. Sci. 3 (2012) 543–550.

[5] X. Ouyang, X. Qiu, H. Lou, D. Yang, Corrosion and scale inhibition properties of sodium lignosulfonate and its potential application in recirculating cooling water system, Ind. Eng. Chem. Res. 45 (2006) 5716–5721, https://doi.org/10.1021/ie0513189.

[6] L. Tang, G. Mu, G. Liu, The effect of neutral red on the corrosion inhibition of cold rolled steel in 1.0 M hydrochloric acid, Corros. Sci. 45 (2003) 2251–2262, https://doi.org/10.1016/S0010-938X(03)00046-5.

[7] G.I. Ramírez-Peralta, U. León-Silva, M.E. Nicho Díaz, M.G. Valladares-Cisneros, Effect of Equisetum arvense extract as corrosion inhibitor of A36 steel in sulfuric acid solution, Mater. Corros. 69 (11) (2018) 1631–1637.

[8] H. Gerengi, M.M. Solomon, S. Öztürk, A. Yıldırım, G. Gece, E. Kaya, Evaluation of the corrosion inhibiting efficacy of a newly synthesized nitrone against St37 steel corrosion in acidic medium: Experimental and theoretical approaches, Mater. Sci. Eng. C. 93 (2018) 539–553, https://doi.org/10.1016/j.msec.2018.08.031.

[9] P. Divya, S. Subhashini, A. Prithiba, R. Rajalakshmi, Tithonia diversifolia flower extract as green corrosion inhibitor for mild steel in acid medium, Mater. Today Proc. 18 (2019) 1581–1591, https://doi.org/10.1016/j.matpr.2019.05.252.

[10] M. Bozorg, T.S. Farahani, G. Mohammadi, J. Neshati, Z. Chaghazardi, Inhibitive Assessment of N- (8-Bromo-3H-Phenoxazin-3-Ylidene) -N , N ′ -Dimethylaminium , as A Novel Corrosion Inhibitor for Mild Steel In 1 . 0 M Hcl, J. Adv. Mater. Process. 2 (2014) 27–38.

[11] M. Kaddouri, S. Rekkab, M. Bouklah, B. Hammouti, a. Aouniti, Z. Kabouche, Experimental study of inhibition of corrosion of mild steel in 1 M HCl solution by two newly synthesized calixarene derivatives, Res. Chem. Intermed. 39 (2012) 3649–3667. https://doi.org/10.1007/s11164-012-0869-2.

[12] T. Douadi, H. Hamani, D. Daoud, M. Al-noaimi, S. Chafaa, Effect of temperature and hydrodynamic conditions on corrosion inhibition of an azomethine compounds for mild steel in 1 M HCl solution, J. Taiwan Inst. Chem. Eng. 71 (2017) 388–404, https://doi.org/10.1016/j.jtice.2016.11.026.

[13] M. Rezaeivala, H. Keypour, Schiff base and non-Schiff base macrocyclic ligands and complexes incorporating the pyridine moiety - The first 50 years, Coord. Chem. Rev. 280 (2014) 203–253, https://doi.org/10.1016/j.ccr.2014.06.007.

[14] H. Jafari, F. mohsenifar, K. Sayin, Corrosion inhibition studies of N, N'-bis(4-formylphenol)-1,2-Diaminocyclohexane on steel in 1 HCl solution acid, J. Taiwan Inst. Chem. Eng. 64 (2016) 314–324.

[15] E. Barmatov, T. Hughes, Degradation of a schiff-base corrosion inhibitor by hydrolysis, and its effects on the inhibition efficiency for steel in hydrochloric acid, Mater. Chem. Phys. 257 (2021) 123758, https://doi.org/10.1016/j.matchemphys.2020.123758.

[16] E.A. Badr, M.A. Bedair, S.M. Shaban, Adsorption and performance assessment of some imine derivatives as mild steel corrosion inhibitors in 1.0 M HCl solution by chemical, electrochemical and computational methods, Mater. Chem. Phys. 219 (2018) 444–460, https://doi.org/10.1016/j.matchemphys.2018.08.041.

[17] M. Rezaeivala, M. Ahmadi, B. Captain, M. Bayat, M. Saeidirad, S. Şahin-Bölükbaşı, B. Yıldız, R.W. Gable, Some new morpholine-based Schiff-base complexes; Synthesis, characterization, anticancer activities and theoretical studies, Inorganica Chim. Acta. 513 (2020) 119935, https://doi.org/10.1016/j.ica.2020.119935.

[18] M. Rezaeivala, R. Golbedaghi, M. Khalili, M. Ahmad, K. Sayin, F. Chalabian, The Different Effects of Metal Ions on the Synthesis of Macroacyclic Compounds: X-ray Crystal Structure, Theoretical Studies, Antibacterial and Antifungal Activities, Russ. J. Coord. Chem. Khimiya. 45 (2019) 142–153, https://doi.org/10.1134/S1070328419020064.

[19] M. Rezaeivala, H. Keypour, S. Salehzadeh, R. Latifi, F. Chalabian, F. Katouzian, Synthesis, characterization and crystal structure of some new Mn(II) and Zn(II) macroacyclic Schiff base complexes derived from two new asymmetrical (N5) branched amines and pyridine-2-carbaldehyde or O-vaniline and their antibacterial properties, J. Iran. Chem. Soc. 11 (2014) 431–440, https://doi.org/10.1007/s13738-013-0315-4.

[20] G. Mohammadi Ziarani, Z. Kheilkordi, F. Mohajer, A. Badiei, R. Luque, Magnetically recoverable catalysts for the preparation of pyridine derivatives: an overview, RSC Adv. 11 (2021) 17456–17477, https://doi.org/10.1039/d1ra02418c.

[21] S. Kalhor, M. Yarie, M. Torabi, M.A. Zolfigol, M. Rezaeivala, Y. Gu, Synthesis of 2-Amino-6-(1 H -Indol-3-yl)-4-Phenylnicotinonitriles and Bis(Indolyl) Pyridines Using a Novel Acidic Nanomagnetic Catalyst via a Cooperative Vinylogous Anomeric-Based Oxidation Mechanism, Polycycl. Aromat. Compd. 42 (7) (2022) 4270–4285.

[22] A. Afkhami, F. Soltani-Felehgari, T. Madrakian, H. Ghaedi, M. Rezaeivala, Fabrication and application of a new modified electrochemical sensor using nano-silica and a newly synthesized Schiff base for simultaneous determination of Cd2+, Cu2+ and Hg2+ ions in water and some foodstuff samples, Anal. Chim. Acta. 771 (2013) 21–30, https://doi.org/10.1016/j.aca.2013.02.031.

[23] M. Prabakaran, S.H. Kim, K. Kalaiselvi, V. Hemapriya, I.M. Chung, Highly efficient Ligularia fischeri green extract for the protection against corrosion of mild steel in acidic medium: Electrochemical and spectroscopic investigations, J. Taiwan Inst. Chem. Eng. 59 (2016) 553–562, https://doi.org/10.1016/j.jtice.2015.08.023.

[24] P. Rugmini Ammal, M. Prajila, A. Joseph, Effective inhibition of mild steel corrosion in hydrochloric acid using EBIMOT, a 1, 3, 4-oxadiazole derivative bearing a 2-ethylbenzimidazole moiety: Electro analytical, computational and kinetic studies, Egypt. J. Pet. 27 (2018) 823–833, https://doi.org/10.1016/j.ejpe.2017.12.004.

[25] P. Rugmini Ammal, M. Prajila, A. Joseph, Physicochemical studies on the inhibitive properties of a 1,2,4-triazole Schiff's base, HMATD, on the corrosion of mild steel in hydrochloric acid, Egypt. J. Pet. 27 (2018) 307–317, https://doi.org/10.1016/j.ejpe.2017.05.002.

[26] S. Deng, X. Li, Inhibition by Jasminum nudiflorum Lindl. leaves extract of the corrosion of aluminium in HCl solution, Corros. Sci. 64 (2012) 253–262, https://doi.org/10.1016/j.corsci.2012.07.017.

[27] A.A. Farag, M.R.N. El-din, The adsorption and corrosion inhibition of some nonionic surfactants on API X65 steel surface in hydrochloric acid, Corros. Sci. 64 (2012) 174–183, https://doi.org/10.1016/j.corsci.2012.07.016.

[28] K. Zhang, B. Xu, W. Yang, X. Yin, Y. Liu, Y. Chen, Halogen-substituted imidazoline derivatives as corrosion inhibitors for mild steel in hydrochloric acid solution, Corros. Sci. 90 (2015) 284–295, https://doi.org/10.1016/j.corsci.2014.10.032.

[29] Z. Tao, G. Liu, Y. Li, R. Zhang, H. Su, S. Li, Electrochemical Investigation of Tetrazolium Violet as a Novel Copper Corrosion Inhibitor in an Acid Environment, ACS Omega 5 (2020) 4415–4423, https://doi.org/10.1021/acsomega.9b03475.

[30] A. Zarrouk, H. Zarrok, R. Salghi, B. Hammouti, F. Bentiss, R. Touir, M. Bouachrine, Evaluation of N-containing organic compound as corrosion inhibitor for carbon steel in phosphoric acid, J. Mater. Environ. Sci. 4 (2013) 177–192.

[31] N. Karki, S. Neupane, D.K. Gupta, A.K. Das, S. Singh, G.M. Koju, Y. Chaudhary, A. P. Yadav, Berberine isolated from Mahonia nepalensis as an eco-friendly and thermally stable corrosion inhibitor for mild steel in acid medium, Arab. J. Chem. 14 (12) (2021) 103423, https://doi.org/10.1016/j.arabjc.2021.103423.

[32] C. Cao, On electrochemical techniques for interface inhibitor research, Corros. Sci. 38 (1996) 2073–2082, https://doi.org/10.1016/S0010-938X(96)00034-0.

[33] M. Amirjan, M. Bozorg, H. Sakiani, Investigation of microstructure and corrosion behavior of IN718 superalloy fabricated by selective laser melting, Mater. Chem. Phys. 263 (2021), 124368, https://doi.org/10.1016/j.matchemphys.2021.124368.

[34] M. Moradi, J. Duan, X. Du, Investigation of the effect of 4, 5-dichloro-2-n-octyl-4-isothiazolin-3-one inhibition on the corrosion of carbon steel in Bacillus sp. inoculated artificial seawater, Corros. Sci. 69 (2013) 338–345, https://doi.org/10.1016/j.corsci.2012.12.017.

[35] M. Lebrini, F. Robert, A. Lecante, C. Roos, Corrosion inhibition of C38 steel in 1M hydrochloric acid medium by alkaloids extract from Oxandra asbeckii plant, Corros. Sci. 53 (2) (2011) 687–695.

[36] M.R. Gholamhosseinzadeh, H. Aghaie, M.S. Zandi, M. Giahi, Rosuvastatin drug as a green and effective inhibitor for corrosion of mild steel in HCl and H2SO4 solutions, J. Mater. Res. Technol. 8 (2019) 5314–5322, https://doi.org/10.1016/j.jmrt.2019.08.052.

[37] D. Quy Huong, T. Duong, P.C. Nam, Effect of the Structure and Temperature on Corrosion Inhibition of Thiourea Derivatives in 1.0 M HCl Solution, ACS, Omega 4 (2019) 14478–14489, https://doi.org/10.1021/acsomega.9b01599.

[38] A.K. Singh, B. Chugh, S. Thakur, B. Pani, H. Lgaz, I.M. Chung, S. Pal, R. Prakash, Green approach of synthesis of thiazolyl imines and their impeding behavior against corrosion of mild steel in acid medium, Colloids Surfaces A Physicochem. Eng. Asp. 599 (2020), 124824, https://doi.org/10.1016/j.colsurfa.2020.124824.

[39] Sudheer, M.A. Quraishi, Quraishi, Thermodynamic and Electrochemical Investigation of Pantoprazole: (RS)-6-(difluoromethoxy)-2- [(3,4-dimethoxypyridin-2-yl)methylsulfinyl]-1H-benzo[d]-imidazole as Corrosion Inhibitor for Mild Steel in Hydrochloric Acid Solution, Arab. J. Sci. Eng. 38 (1) (2013) 99–109.

[40] M. Bozorg, T. Shahrabi Farahani, J. Neshati, G. Mohammadi Ziarani, Z. Chaghazardi, P. Gholamzade, F. Ektefa, Corrosion inhibitive behavior of 7-hydroxyphenoxazone on mild steel in 1.0 M HCl, Res. Chem. Intermed. (2014), https://doi.org/10.1007/s11164-014-1722-6.

[41] A. Kosari, M. Momeni, R. Parvizi, M. Zakeri, M.H. Moayed, A. Davoodi, H. Eshghi, Theoretical and electrochemical assessment of inhibitive behavior of some thiophenol derivatives on mild steel in HCl, Corros. Sci. 53 (2011) 3058–3067, https://doi.org/10.1016/j.corsci.2011.05.009.

[42] B. Ramezanzadeh, S.Y. Arman, M. Mehdipour, B.P. Markhali, Applied Surface Science Analysis of electrochemical noise (ECN) data in time and frequency domain for comparison corrosion inhibition of some azole compounds on Cu in 1 . 0 M H 2 SO 4 solution, Appl. Surf. Sci. 289 (2014) 129–140. https://doi.org/10.1016/j.apsusc.2013.10.119.

[43] M. Lebrini, F. Bentiss, N.E. Chihib, C. Jama, J.P. Hornez, M. Lagrenée, Polyphosphate derivatives of guanidine and urea copolymer: Inhibiting corrosion effect of Armco iron in acid solution and antibacterial activity, Corros. Sci. 50 (2008) 2914–2918, https://doi.org/10.1016/j.corsci.2008.07.003.

[44] F. Bentiss, C. Jama, B. Mernari, H. El Attari, L. El Kadi, M. Lebrini, M. Traisnel, M. Lagrenée, Corrosion control of mild steel using 3,5-bis(4-methoxyphenyl)-4-amino-1,2,4-triazole in normal hydrochloric acid medium, Corros. Sci. 51 (2009) 1628–1635, https://doi.org/10.1016/j.corsci.2009.04.009.

[45] A.Y. Musa, R.T.T. Jalgham, A. Bakar, Molecular dynamic and quantum chemical calculations for phthalazine derivatives as corrosion inhibitors of mild steel in 1 M HCl, Corros. Sci. 56 (2012) 176–183, https://doi.org/10.1016/j.corsci.2011.12.005.

[46] A. Ghanbari, M.M. Attar, M. Mahdavian, Corrosion inhibition performance of three imidazole derivatives on mild steel in 1 M phosphoric acid, Mater. Chem. Phys. 124 (2010) 1205–1209, https://doi.org/10.1016/j.matchemphys.2010.08.058.

[47] S. Chen, S. Chen, B. Zhu, C. Huang, W. Li, Magnolia grandi fl ora leaves extract as a novel environmentally friendly inhibitor for Q235 steel corrosion in 1 M HCl : Combining experimental and theoretical researches, J. Mol. Liq. 311 (2020), 113312, https://doi.org/10.1016/j.molliq.2020.113312.

[48] F. Bentiss, Thermodynamic characterization of metal dissolution and inhibitor adsorption processes in mild steel / hydrochloric acid system, Corros. Sci. 47 (2005) 2915–2931, https://doi.org/10.1016/j.corsci.2005.05.034.

[49] C. Xu, W. Li, B. Tan, X. Zuo, S. Zhang, Adsorption of Gardenia jasminoides fruits extract on the interface of Cu / H 2 SO 4 to inhibit Cu corrosion : Experimental and theoretical studies, J. Mol. Liq. (2021), 116996, https://doi.org/10.1016/j.molliq.2021.116996.

[50] Y. Qiang, S. Zhang, L. Wang, Understanding the adsorption and anticorrosive mechanism of DNA inhibitor for copper in sulfuric acid, Appl. Surf. Sci. 492 (2019) 228–238, https://doi.org/10.1016/j.apsusc.2019.06.190.

[51] S.E. Hachani, Z. Necira, D.E. Mazouzi, N. Nebbache, Understanding the Inhibition of Mild Steel Corrosion by Dianiline Schiff Bases : a DFT Investigation, Acta Chim. Slov. 65 (2018) 183–190, https://doi.org/10.17344/acsi.2017.3803.

[52] M.S. Çelik, Ş.A. Çetinus, A.F. Yenidünya, S. Çetinkaya, B. Tüzün, Biosorption of Rhodamine B dye from aqueous solution by Rhus coriaria L. plant: Equilibrium, kinetic, thermodynamic and DFT calculations, J. Mol. Struct. 1272 (2023) 134158, https://doi.org/10.1016/j.molstruc.2022.134158.

[53] M. Chalkha, A. Ameziane el Hassani, A. Nakkabi, B. Tüzün, M. Bakhouch, A. T. Benjelloun, M. Sfaira, M. Saadi, L. El Ammari, M. El Yazidi, Crystal structure, Hirshfeld surface and DFT computations, along with molecular docking investigations of a new pyrazole as a tyrosine kinase inhibitor, J. Mol. Struct. 1273 (2023), 134255, https://doi.org/10.1016/j.molstruc.2022.134255.

[54] A. Mermer, M. Volkan Bulbul, S. Mervenur Kalender, I. Keskin, B. Tuzun, O. Emre Eyupoglu, Benzotriazole-oxadiazole hybrid Compounds: Synthesis, anticancer Activity, molecular docking and ADME profiling studies, J. Mol. Liq. 359 (2022), 119264, https://doi.org/10.1016/j.molliq.2022.119264.